

## SECONDARY EMISSION FROM THIN METAL FOILS BOMBARDED WITH 70-MEV ELECTRONS

S. A. Blankenburg, J. K. Cobb and J. J. Muray  
Stanford Linear Accelerator Center  
Stanford University, Stanford, California

### Summary

The secondary electron emission coefficient from several elements in the form of thin foils has been measured using 70 MeV electrons as bombarding particles.

Using foils with different atomic numbers, it was found that the secondary emission coefficient per target electron in the metal is noticeably larger for light elements, especially in cases of beryllium and aluminum. This indicates that metal oxide on the foil surface (Malter effect) is playing a dominant role in the secondary emission of these metals.

For other metals, the experimental results seem to indicate a relatively small variation in the secondary emission coefficient per target electron, less than that predicted by V. J. Vanhuysse and R. E. Van de Vijver, but with the same general behavior.

The lack of thickness dependence in the case of tantalum foils is in agreement with the extensive experimental work of B. Plansky and with the theoretical treatment of the secondary emission by Aggson.

The secondary electron emission coefficients will be given for the measured foils and the experimental values will be compared with the existing theories. Finally, the construction of a bakeable secondary emission current monitor will be described.

### Introduction

The purpose of this paper is to summarize the experimental results on the secondary electron emission yields from thin metal foils bombarded with a high energy electron beam. This study was started as a search for a stable and accurate beam current monitor for high energy (10 MeV - 20 GeV) and high intensity ( $10^{-11}$  -  $10^{-4}$  amps) electron beams.

### Experimental Results

#### Experimental Setup

For the experimental work to study the secondary electron emission properties of thin metal foils bombarded with electrons of 70 MeV of energy, the Stanford Mark IV linear accelerator was used. The configuration of the apparatus used in the experiment is shown schematically in Fig. 1. The electron beam from the accelerator was energy analyzed (energy resolution  $\approx 1\%$ ) by a magnetic deflection system, passed through two SEM's built

from different foils, and finally collected in a Faraday cup. The efficiency ( $\gamma$ ) of the different foils is given as the ratio of charge integrated on a condenser to the charge collected in the Faraday cup. The Faraday cup was designed to catch more than 99% of the electrons in the beam.

The experiments were run under high vacuum conditions, usually  $3 \times 10^{-7}$  torr or better. The foils in the monitor were cleaned and the whole monitor, built from stainless steel, was baked out under vacuum for at least 12 hours.

#### Yield Dependence on Atomic Number

Twelve different foils have been measured in this secondary emission study: Beryllium, aluminum, titanium, 320 stainless steel, nickel, copper, molybdenum, rhodium, silver, tantalum, wolfram, and gold. The results are displayed in Fig. 2 which shows the efficiency of each element as compared to the efficiency of gold. The upper curve shows the theoretical prediction of V. J. Vanhuysse and R. E. Van de Vijver.<sup>1</sup> A more detailed comparison of the experimental results with the theoretical predictions will be treated later. The interesting aspects of secondary emission are more clearly seen in Fig. 3. Here the measured relative yields (Efficiency X/Efficiency Au) are divided by the electron density  $\delta N_0 Z/A$  in the foils, where  $N_0$  is Avogadro's number,  $\delta$  is the density of the foil,  $Z$  is the atomic number, and  $A$  is the atomic weight. This curve shows the efficiency of secondary electron emission per target electron. The light elements, especially beryllium and aluminum, are noticeably more efficient elements than theory predicts. Beginning with titanium and for  $Z$  higher than titanium, the efficiency is in good agreement with theory. Because both beryllium and aluminum have oxide coatings under normal conditions, this may indicate that the oxide is playing a dominant role in the secondary emission of these metals. Except for these two metal foils, however, the experimental results seem to indicate a relatively small variation in efficiency per electron among elements, less than that predicted by theory but with the same general behavior.

#### Thickness Dependence

The secondary emission yield was measured for tantalum foils 1.0 mil and 2.4 mils thick. No significant difference was observed in their secondary emission for collection voltages between 1 and 500 volts. This is a direct contradiction to the theory of Vanhuysse and Van de Vijver, which predicts that the total yield of a given foil goes as

$Y = F_1$  (energy, metal constants) +  $F_2$  (energy, metal constants)(thickness) $^2$  where  $F_2$  is larger than  $F_1$  for all measured elements. For tantalum, this theory predicts that

$$\frac{Y_{Ta}(2.4 \text{ mil})}{Y_{Ta}(1.0 \text{ mil})} = 1.48$$

This lack of thickness dependence is in agreement with the extensive experimental works of B. Plansky<sup>2</sup> on aluminum and with the theoretical treatment of secondary electron emission by Th. L. Aggson.<sup>5</sup>

#### Surface Effects

To investigate the effect of the beam on the surface layer of the foil, the yield was measured with different beam currents and varying collector voltage. In these runs the foil surface was "baked" out for an hour by beams of different currents values and the yield was recorded as a function of the collection voltage. Figure 4 shows the relative efficiency as a function of the collection voltage after an hour of baking with different intensity beams. It is evident from this figure that the yield changed at low collection voltage values; i.e., the energy spectrum of the secondary electrons is altered by the change in the surface layer, but the high voltage yield values did not change appreciably. This indicates that the low energy part of the secondary electron emission spectrum is a very sensitive function of the characteristics of the surface layer, but it does not influence the efficiency of the SEM when the collection voltage is high enough.

Figures 5 and 6 give the variation in efficiency as a function of collection voltage divided by the corresponding efficiency of gold and aluminum at the same voltage. These results were all obtained at energies around 70 MeV with average currents between 3 and 5  $\mu\text{A}$ . By taking the derivatives of these curves one can determine the energy spectrum of the secondary electrons from different metal foils as compared to gold and aluminum. Most of the electrons seem to be emitted with energies below 30 eV, which is what one should expect if the secondary emission is truly a surface phenomena, as seems to follow from the thickness dependence measurements.

There was no observed variation in the efficiency of secondary electron emission with currents ranging from 0.1  $\mu\text{A}$  to 20  $\mu\text{A}$ . It was difficult to get consistent data below 0.1  $\mu\text{A}$  because of the long integrating times involved and the galvanic currents of this magnitude observed on the Faraday cup itself from the cooling water. One of the most interesting aspects of the secondary emission is the small decrease in efficiency of the collection process from a maximum with increasing collection voltage. This effect has been explained by Aggson as a manifestation of the Malter effect due to the surface contamination by vacuum pump oils and the oxide coatings. In this study all the metal foils showed this effect to some degree, although the

cleanest metal surfaces, particularly molybdenum, gold and tantalum, show exactly the same effect when compared to each other in the same run. For example, in Fig. 5 the efficiency of molybdenum foil divided by the efficiency of the gold foil in the same SEM during the same run remains constant above a 20-volt collection voltage. This would appear to indicate either that the effect is due to the experimental setup, or that both metals were contaminated exactly the same, possibly by vacuum pump oil.

#### High Energy Secondary Electrons

The properties of the high energy secondary electrons (knock-on electrons or delta rays) emitted from metal foils have been investigated by Shatas, Marshall and Pomerantz<sup>4</sup> and recently by B. Plansky.<sup>2</sup> It was found that the percentage of the high energy secondary electrons in the total yield depends on the thickness as  $t^2$ , and it is not influenced by the surface condition of the emitting foil. In this experiment the fraction of the high energy electrons emitted from the foil was estimated from the following measurements. On a three-element SEM the collector voltages were applied with three different polarities, as shown in Figs. 7a, 7b, and 7c. Figure 7a shows the normal operation of a three-element SEM; in this case the electron collection efficiency is the largest and the measured yield divided by two gives the efficiency per active foil surface.  $I_F$  is the high energy component of the secondary emission current emitted by foil and unaffected by the field.

A fraction  $\alpha$  of this high energy secondary electron current is stopped by the following foil. The arrows on Fig. 7 show the directions of the electron currents and the letters F and B refer to the front or back side emission currents relative to the beam direction.

Figure 7b shows the secondary electron currents when the first foil was negative with respect to the center and the third was at positive potential. Without high energy components in the emission, one would expect zero efficiency with this polarity similar to the case where the first foil was positive and the third was negative with respect to the center foil (Fig. 7c). The experimental results from these measurements for Zr and Rd are shown in Fig. 8, where the electron collection efficiency on the center foil is plotted versus the collection voltage. It can be seen from these curves that the value of the collection voltage does not markedly change the collection efficiency in the low voltage region as it does in the case of the low energy component. Using the measured electron collection efficiency, the fraction of the high energy component in the total electron collection efficiency can be estimated as

$$R_{\text{coll}} = \frac{1}{2} \left( \frac{Y_{Rd+-} + Y_{Rd--}}{Y_{Rd}} \right) \approx 3.6\%$$

This high energy electron collection efficiency might be interpreted as the lower limit for the

ratio of the high to low energy electrons in the total secondary electron emission.

#### Construction of a Low Pressure Bakeable Secondary Emission Current Monitor

In this section we would like to describe briefly the construction of a bakeable secondary electron emission current monitor<sup>5</sup> (SEM). This type of current monitor is extensively used for linear accelerators because it has a very large linear current range, as opposed to the ionization chamber which saturates above a certain beam current (depending on the pressure). To achieve stable operation with the SEM over long periods of time, one should use extremely clean metal foils.

Thin foils such as Ni, Rd, Ag, W, Au (see Fig. 2) give very stable operation in current monitors; however, in certain experiments they cannot be used because the  $\gamma$ -background from the bremsstrahlung and the multiple scattering of the electrons in the high Z foils are intolerable. In this case, nickel, silver or gold plated aluminum foils can be used. Molecular layers from the residual gas (especially for Al foils) can influence the efficiency of the SEM in the first hour of operation. To avoid instability in the operation of the SEM, one can design a bakeable low pressure monitor.

The mechanical layout of the secondary electron emission monitor which was used for this experiment is such that all the internal parts are mounted on the large vacuum flange. The target foils are mounted on circular aluminum frames; wire springs hold the target foils rigidly in the frames. The frame itself is mounted on four round bars. Ceramic washers insulate the frames against each other and also against the round bars. The frames have small clamps attached at the circumference which serve as electrical connectors. The electrical connection from the outside of the chamber to the foils is through the ceramic feedthroughs mounted at the large flange. The electrical conductor is connected to the frames with the attached clamping devices. At either side of the vacuum chamber an aluminum window is attached. If it is necessary to gain access to some interior parts of the chamber, it is only necessary to dismount the large vacuum flange; no windows must be dismantled.

Figure 9 shows the mechanical construction of the current monitor and in Fig. 10 a photograph of the device is shown.

In the overall arrangement, the ion pump is directly connected to the vacuum chamber. The vacuum valve as shown in the photograph is for the connection of the roughing pump, which can be either a piston pump or a sorption pump. It is not necessary to replace the copper gasket of the large vacuum flange when disassembling the flange. The gasket can be reused for at least 15 to 20 assembly-disassembly cycles.

The construction method of the window is shown in Fig. 11. In order to prevent wrinkles in the foil and to insure uniform tension along the sealing

line, an incline of  $8^\circ$  was machined on the flange. The seal ring, which is made from copper; has the configuration as shown. The seal force applied to the copper ring is approximately  $1/4$  inch smaller in diameter than the seal line of the copper ring against the aluminum foil. When applying a sealing force, prestressing of the foil occurs, which in turn reduces the amount of cave-in when vacuum is applied at one side of the window. Experiments showed that an  $8^\circ$  angle is the best suitable configuration for tightening the bolts, in order to prevent uneven tension along the seal edge. The window was vacuum-tight when the vacuum was applied on either side of the foil. Vacuum achieved in a small vacuum chamber with two windows of this configuration was in the  $10^{-9}$  torr range. The upper seal edge was  $2-3/4$ -inches in diameter, 8 bolts of  $1/4$ -inch diameter were used, and the torque applied to each bolt was 6 foot-pounds. Because this was the easiest and simplest method for manufacturing, this method was adopted for use with the secondary electron emission monitor.

The copper ring needs no replacing after taking the seal apart and reassembling it. The reassembling-and-taking-apart procedure was carried out six times without replacing the copper ring, and each time a vacuum-tight seal was achieved.

#### List of References

1. V.J. Vanhuyse and R.E. Van de Vijver, Nuc. Instr. and Meth. 15, 63 (1962).
2. B. Planskoy, Nuc. Instr. and Meth. 24, 172 (1963).
3. Th. L. Aggson, Report IAL-1028, Laboratoire de l'accélérateur linéaire, Orsay, France (1962).
4. R.A. Shatas, J.F. Marshall and M.A. Pomerantz, Phys. Rev. 96, 1199 (1954).
5. H. Hauser and J.J. Muray, Internal Report, Stanford Linear Accelerator Center, Stanford University, Stanford, California (1963).

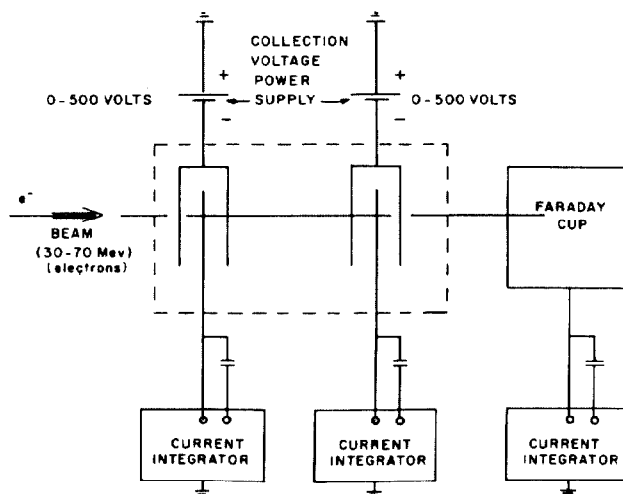


Fig. 1. Schematic of Experimental Setup.

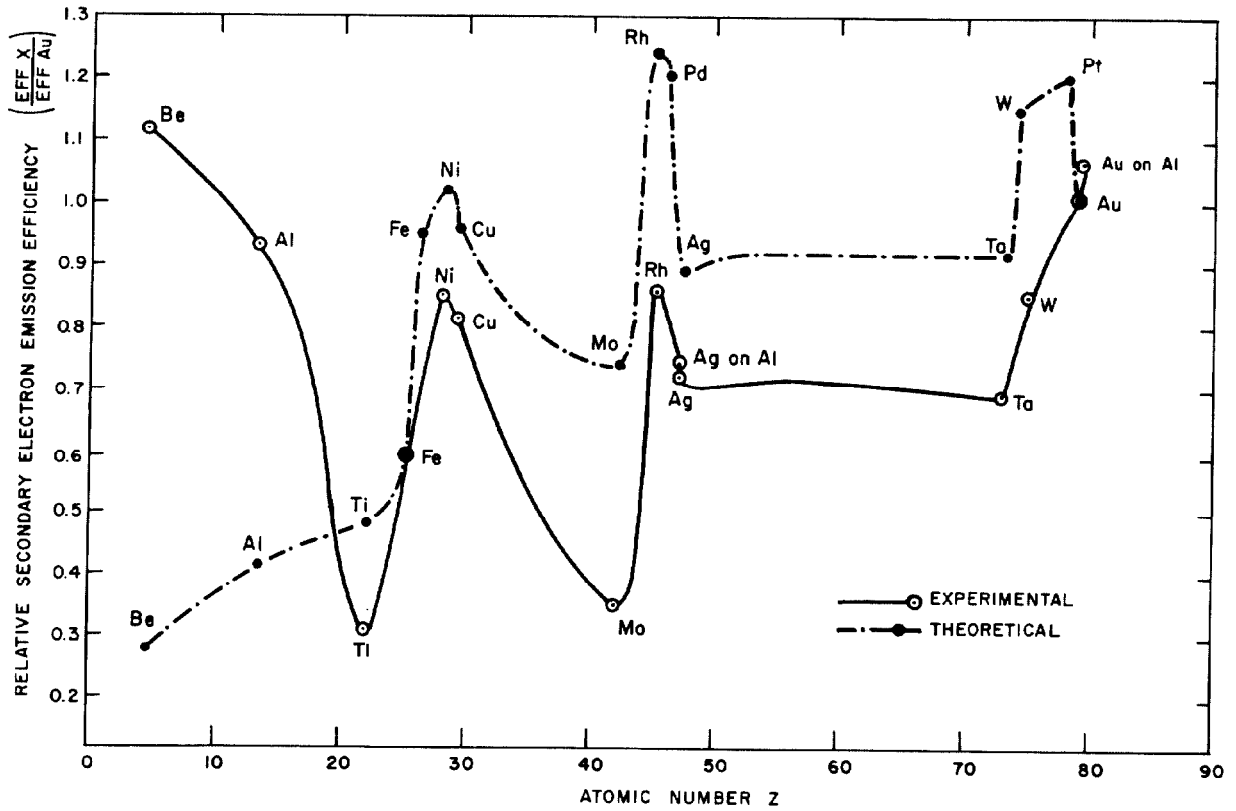
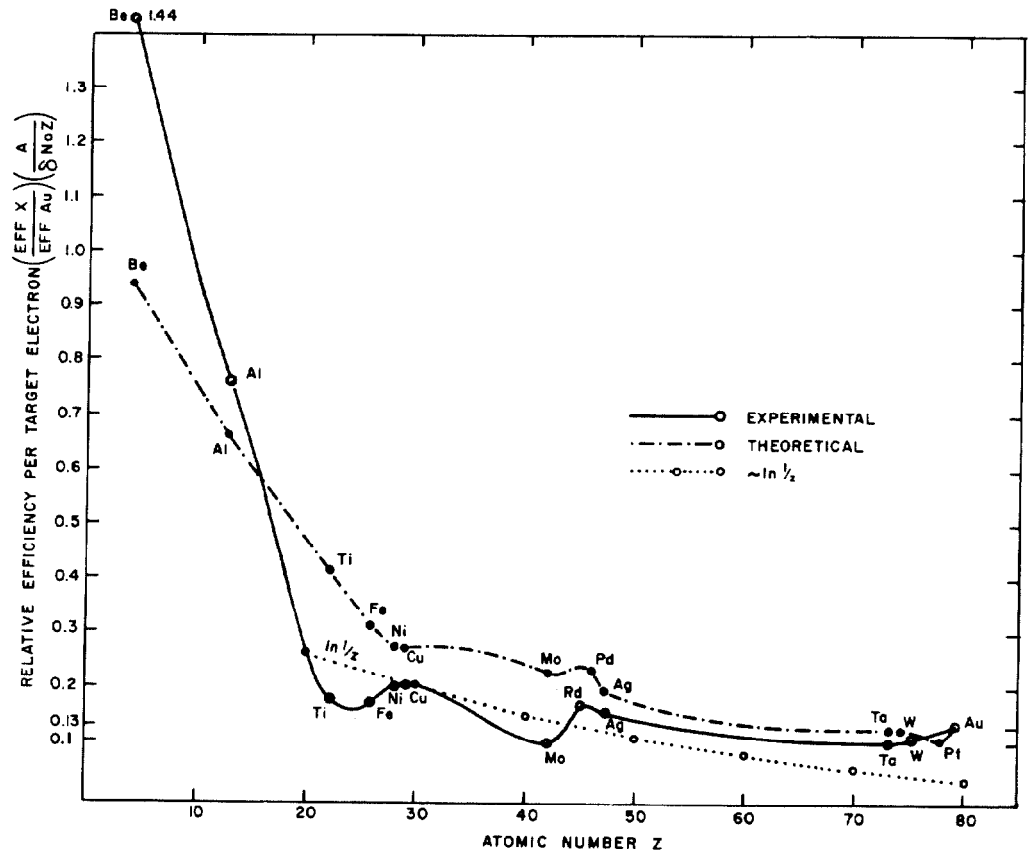


Fig. 2. Relative Efficiency vs. Atomic Number.

Fig. 3. Relative Efficiency per Target Electron vs. Atomic Number.



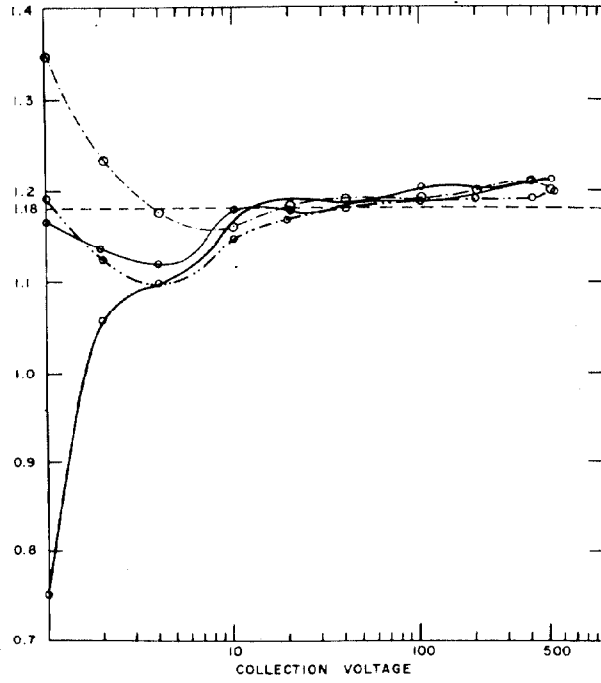


Fig. 4.  $Y_{Be}/Y_{Al}$  vs. Collection Voltage at 74 MeV.

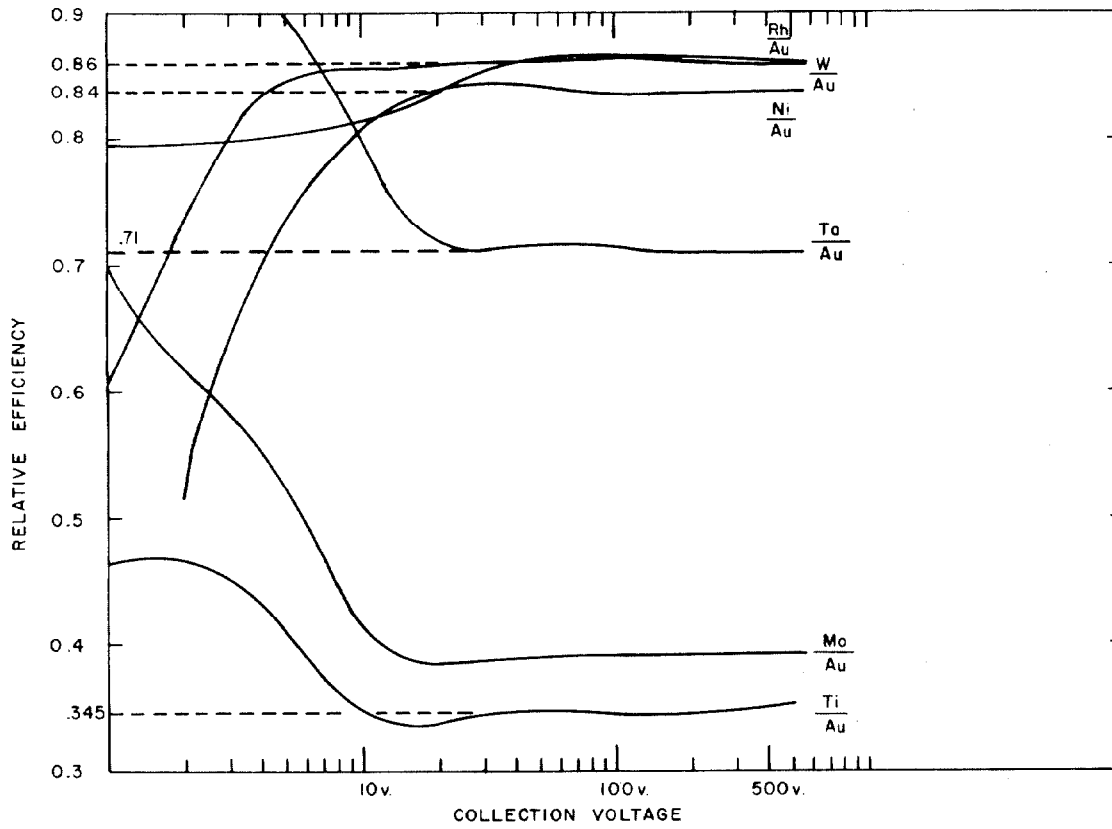


Fig. 5. Relative Efficiency vs. Collection Voltage. Primary Electron Energy 70 MeV.

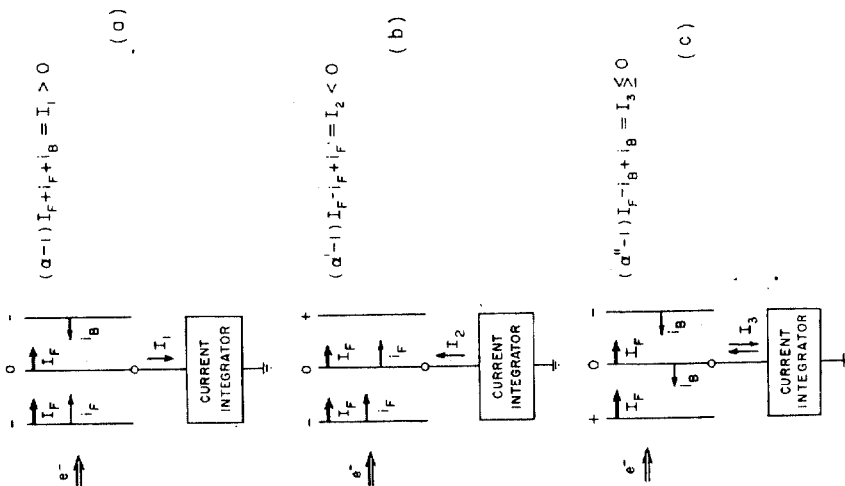


Fig. 7. Arrangements for Measuring the High Energy Components in the Secondary Electron Emission.

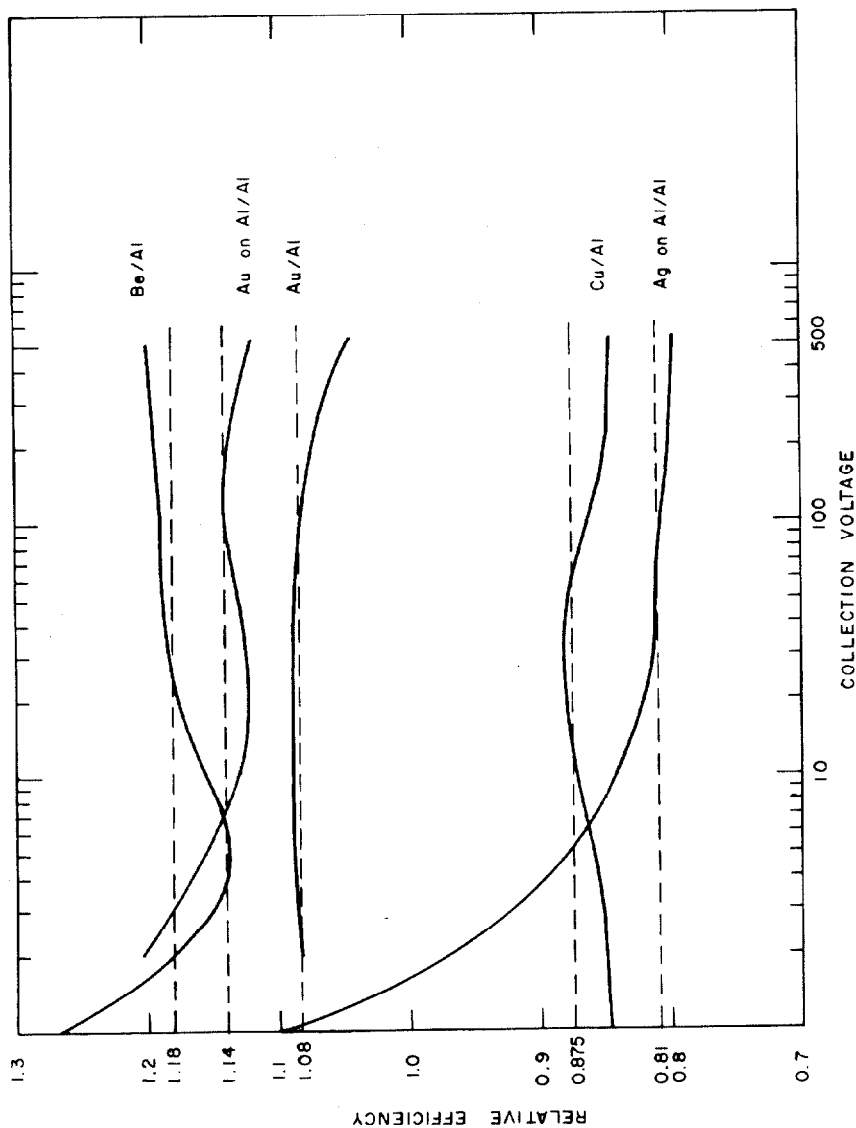


Fig. 6. Relative Efficiency vs. Collection Voltage.

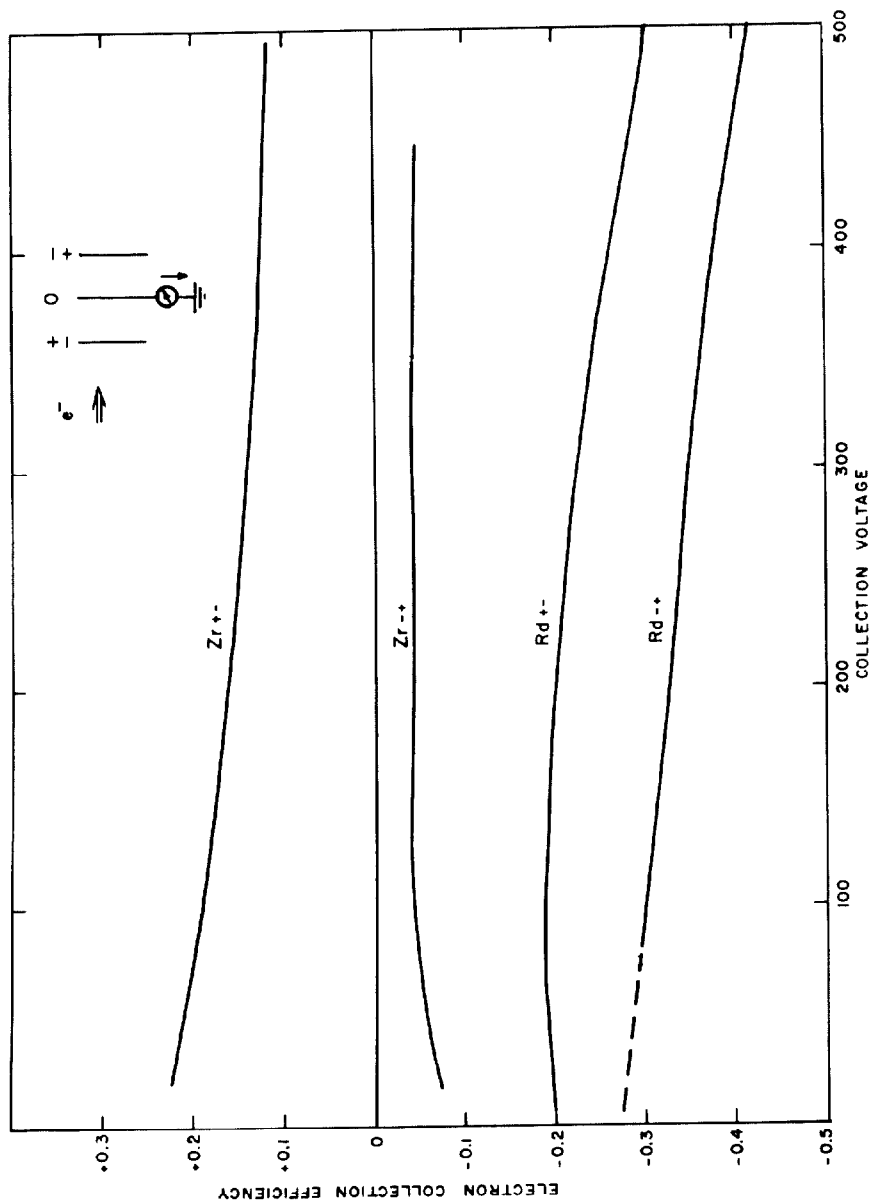


Fig. 8. Electron Collection Efficiency vs. Collection Voltage.

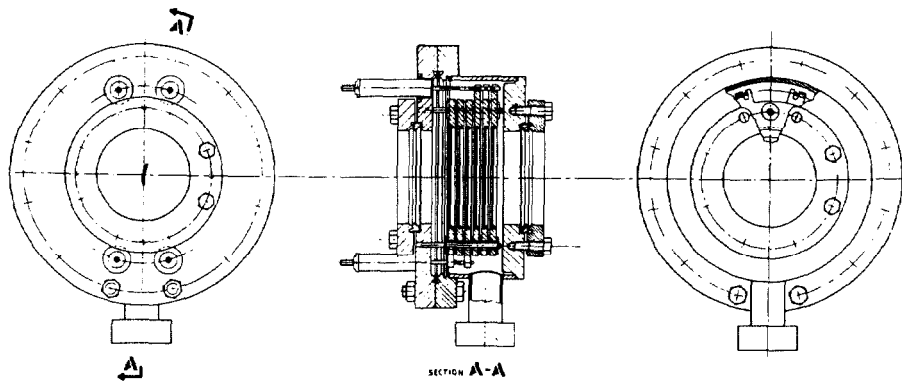


Fig. 9. Diagram of Secondary Emission Beam Current Monitor.

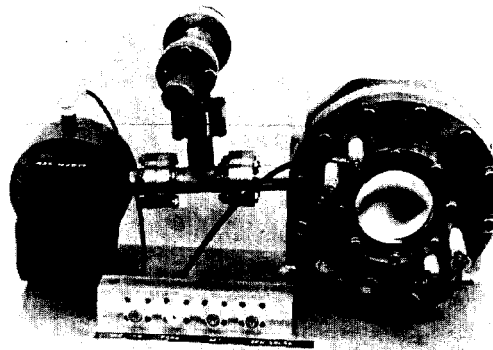


Fig. 10. Photo of Secondary Emission Beam Current Monitor.

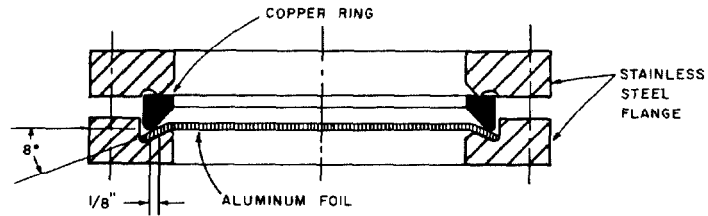


Fig. 11. Window Construction.